AGU PUBLICATIONS

JGR

Journal of Geophysical Research: Atmospheres

RESEARCH ARTICLE
10.1002/2017JD027459

Mr. W. Kuster has retired and worked on this manuscript as unaffiliated co-author.

Key Points:
- An expanded data set of hydrocarbons in ambient air in the Los Angeles basin is presented and analyzed
- For reactive alkenes, removal by ozone and nitrate radicals at night is important in addition to their removal by hydroxyl radicals during the day, which complicates determining the composition of emissions
- After correction for chemical removal, the composition of reactive alkene emissions is consistent with a source from motor vehicles

Supporting Information:
- Supporting Information S1

Correspondence to:
J. A. de Gouw,
joost.degouw@colorado.edu

Citation:
de Gouw, J. A., Gilman, J. B., Kim, S.-W., Lerner, B. M., Isaacman-VanWertz, G., McDonald, B. C., … Stutz, J. (2017). Chemistry of volatile organic compounds in the Los Angeles basin: Nighttime removal of alkenes and determination of emission ratios. *Journal of Geophysical Research: Atmospheres*, *122*, 11,843–11,861. https://doi.org/10.1002/2017JD027459

Received 18 JUL 2017
Accepted 26 SEP 2017
Accepted article online 30 SEP 2017
Published online 2 NOV 2017

Chemistry of Volatile Organic Compounds in the Los Angeles basin: Nighttime Removal of Alkenes and Determination of Emission Ratios

J. A. de Gouw[1,2], J. B. Gilman[2], S.-W. Kim[1,2], B. M. Lerner[1,2,3], G. Isaacman-VanWertz[4], B. C. McDonald[1,2], C. Warneke[1,2], W. C. Kuster[2], B. L. Lefer[5,6], S. M. Griffith[7], S. Dusanter[8], P. S. Stevens[9], and J. Stutz[10]

[1]Cooperative Institute for Research in Environmental Sciences, University of Colorado Boulder, Boulder, CO, USA, [2]Earth System Research Laboratory, National Oceanic and Atmospheric Administration, Boulder, CO, USA, [3]Now at Aerodyne Research, Billerica, MA, USA, [4]Department of Civil and Environmental Engineering, Virginia Polytechnic Institute and State University, Blacksburg, VA, USA, [5]Now at NASA Earth Science Division, Washington, DC, USA, [6]Department of Earth and Atmospheric Sciences, University of Houston, Houston, TX, USA, [7]Department of Chemistry, Hong Kong University of Science and Technology, Hong Kong, [8]Département Sciences de l'Atmosphère et Génie de l'Environnement, IMT Lille Douai, University of Lille, Lille, France, [9]School of Public and Environmental Affairs, Indiana University, Bloomington, IN, USA, [10]Department of Atmospheric and Oceanic Sciences, University of California, Los Angeles, CA, USA

Abstract We reanalyze a data set of hydrocarbons in ambient air obtained by gas chromatography-mass spectrometry at a surface site in Pasadena in the Los Angeles basin during the NOAA California Nexus study in 2010. The number of hydrocarbon compounds quantified from the chromatograms is expanded through the use of new peak-fitting data analysis software. We also reexamine hydrocarbon removal processes. For alkanes, small alkenes, and aromatics, the removal is determined by the reaction with hydroxyl (OH) radicals. For several highly reactive alkenes, the nighttime removal by ozone and nitrate (NO_3) radicals is also significant. We discuss how this nighttime removal affects the determination of emission ratios versus carbon monoxide (CO) and show that previous estimates based on nighttime correlations with CO were too low. We analyze model output from the Weather Research and Forecasting-Chemistry model for hydrocarbons and radicals at the Pasadena location to evaluate our methods for determining emission ratios from the measurements. We find that our methods agree with the modeled emission ratios for the domain centered on Pasadena and that the modeled emission ratios vary by 23% across the wider South Coast basin. We compare the alkene emission ratios with published results from ambient measurements and from tunnel and dynamometer studies of motor vehicle emissions. We find that with few exceptions the composition of alkene emissions determined from the measurements in Pasadena closely resembles that of motor vehicle emissions.

Plain Language Summary We report new measurements of hydrocarbons in ambient air in the Los Angeles basin. Chemical reactions between hydrocarbons and nitrogen oxides form ozone and fine particles, two important pollutants in Los Angeles smog. It is therefore important to understand hydrocarbon emission sources. In this work, we derive the composition of hydrocarbon emissions using ambient measurements at Pasadena in 2010. The study is complicated due to rapid chemical reactions that remove hydrocarbons in between the time of emission and measurement. After correcting for this chemistry, it is shown that the composition of reactive alkenes agrees closely with those emitted from motor vehicles.

1. Introduction

The emissions of reactive hydrocarbons to the atmosphere and their photo-oxidation in the presence of nitrogen oxides lead to the formation of secondary pollutants like ozone (Carter, 1994; Derwent et al., 1996) and fine particles (Odum et al., 1997). To study these processes in quantitative detail, it is essential to accurately describe hydrocarbon emissions, both from anthropogenic and natural sources. Anthropogenic hydrocarbon emission inventories are typically constructed "bottom-up" by adding the emissions from all known sources in a region. Such inventories have been evaluated using "top-down" methods that use measurements in ambient air. Emission fluxes can be experimentally determined using a variety of methods including eddy covariance (Karl et al., 2009), mass balance (de Gouw et al., 2009), and inverse modeling (Miller et al., 2008). Other evaluations have compared the composition of emissions between the

inventory and measurements by describing emission ratios versus more inert compounds like carbon monoxide (CO) (Borbon et al., 2013; Warneke et al., 2007). Several studies have reported large discrepancies in anthropogenic hydrocarbon inventories with important implications for ozone chemistry (de Gouw et al., 2015; Petron et al., 2012; Ryerson et al., 2003; Warneke et al., 2007).

To determine anthropogenic hydrocarbon emissions from ambient measurements, the chemical removal of reactive compounds needs to be considered. Reactive hydrocarbons are removed on time scales of hours or less. Most air masses in large cities will contain the combined emissions from a range of sources, some close to the sampling site and others much further away. Reactive hydrocarbons can be removed in between the times of emission and sampling, and other compounds can be formed as a result. To separate the effects of emissions and chemical transformations, various approaches have been attempted. Measurements made during the morning have been used to determine emissions under the assumption that morning rush-hour emissions dominate at that time and that chemistry is inefficient (Parrish et al., 2012). Nighttime measurements have been used to determine the composition of emissions for the same reasons (Borbon et al., 2013). Others have used hydrocarbon ratios to estimate the exposure of sampled air masses to hydroxyl (OH) radicals and determine the emissions by extrapolation to zero OH exposure (de Gouw et al., 2005; Warneke et al., 2007).

In this paper, we study the emissions of anthropogenic hydrocarbons in the Los Angeles basin using measurements made by gas chromatography-mass spectrometry (GC-MS) in Pasadena during the California Nexus (CalNex) study in 2010. Hydrocarbon emission ratios from this data set have been quantified previously (Borbon et al., 2013). Since then, the development of new data analysis software enabled the quantification of several additional hydrocarbons from the chromatograms (Lerner et al., 2017) and the data set has been extended with several branched and cyclic alkanes, alkenes, and oxygenated compounds. In addition, we reevaluate previously reported emissions for reactive alkenes. We will show that nighttime chemical removal of reactive alkenes in urban air led to an underestimate of their emissions in our previous work. We evaluate our methods for determining the composition of hydrocarbon emissions from ambient measurements by analyzing the output from the Weather Research and Forecasting-Chemistry model (WRF-Chem) for Pasadena using the exact same methods as used for the ambient measurements. Finally, we compare the new results for alkene emissions in urban air with those from ambient measurements (Baker et al., 2008; Borbon et al., 2013; Schneidemesser et al., 2010; Warneke et al., 2007; Yuan et al., 2012) and from tunnel (Gentner et al., 2013; Kirchstetter, Singer, Harley, Kendall, & Hesson, 1999; Kirchstetter, Singer, Harley, Kendall, & Traverse, 1999; Lough et al., 2005) and dynamometer studies (May et al., 2014; Schauer et al., 2002) of motor vehicle emissions, and discuss the implications for ozone chemistry.

2. Methods

2.1. Measurement Location and Meteorology

Measurements were made on the campus of the California Institute of Technology in Pasadena from 15 May through 15 June 2010. Figure S1 in the supporting information shows a map of the Los Angeles basin with the location of the ground site indicated by the red marker. Also shown are the diurnal variations in measured wind direction and speed. During the day, the prevailing wind direction was from the Southwest, bringing air masses from the Pacific Ocean to the site that carried emissions from the western part of the LA basin including downtown Los Angeles. At night, winds were low and variable, and the site was more sensitive to emissions from a smaller area centered on Pasadena. Examples of sampling footprints are given elsewhere (Hayes et al., 2013) (supporting information).

2.2. Trace Gas Measurements

A large set of alkanes, alkenes, aromatics, and oxygenated VOCs was measured using a two-channel in situ gas chromatography-mass spectrometry instrument (GC-MS) (Gilman et al., 2010). The GC-MS collected one 5 min sample every 30 min. Since our earlier analysis of this data set (Borbon et al., 2013), several additional compounds were quantified from the chromatograms using newly developed peak fitting software (Lerner et al., 2017). This includes several straight-chain, branched, and cyclic alkanes, reactive alkenes, and oxygenated compounds. The new hydrocarbon measurements are presented in this paper. The new oxygenated compound measurements will be presented in a future publication.

Additional chemical measurements used in this analysis included carbon monoxide (CO) by VUV resonance fluorescence (Gerbig et al., 1999), ozone by NO chemiluminescence, OH radicals by laser-induced fluorescence (Griffith et al., 2016), and NO_3 radicals by long-path differential optical absorption spectroscopy (LP-DOAS) (Tsai et al., 2014). Figure S2 summarizes the times each of these measurements were operational. All additional measurements are averaged onto the sampling times of the GC-MS for the purpose of this analysis unless otherwise noted.

2.3. WRF-Chem Model

Output from the Weather Research and Forecasting-Chemistry (WRF-Chem) model is used to evaluate our analysis methods that separate the effects of emissions, transport, and chemical transformations from the measurement data. The model grid configuration and the physical and chemical options used in WRF-Chem have been described previously (Kim et al., 2016) except for the use of the 2011 National Emissions Inventory (NEI-2011) for anthropogenic VOC emissions: NEI-2005 was used previously, and we adopt the updated anthropogenic VOC emissions from NEI-2011 in this study (Ahmadov et al., 2015). Emissions of NO_x and CO used for the model simulations in this study are identical to those used previously (Kim et al., 2016) and are an expansion of the fuel-based inventory for motor vehicle emissions (McDonald et al., 2012, 2013, 2014).

A brief description of the model and the simulations is given here. We use version 3.4.1 of WRF-Chem (Grell et al., 2005). The nested domain of the WRF-Chem model covers the state of California at 4×4 km^2 horizontal resolution. The model has 60 vertical levels with ~50 m thickness up to 4 km above ground level and coarser vertical resolution at higher levels. The first model level where the mixing ratios of chemical species are calculated is ~25 m. The simulations are conducted for the measurement period analyzed in this study. The meteorological initial and boundary conditions are based on National Centers for Environmental Prediction Global Forecast System data. The global model Model for OZone and Related chemical Tracers (Emmons et al., 2010) is used for initial and boundary conditions for the mother domain of WRF-Chem. Biogenic emissions are based on the Biogenic Emissions Inventory System version 3.13, and emissions from urban vegetation (Scott & Benjamin, 2003) are added. The chemical mechanism is based on the Regional Atmospheric Chemistry Mechanism (Stockwell et al., 1997) with ~30 updated reaction rate coefficients (Kim et al., 2009). The model performance for meteorology and chemical species for the CalNex period was evaluated previously using several of the CalNex data sets (Kim et al., 2016).

2.4. Reaction Rate Coefficients

Rate coefficients for the reactions of hydrocarbons with OH, ozone, and NO_3 radicals are needed throughout this manuscript. In all cases, the rate coefficients at 298 K are used, rather than a temperature-dependent rate coefficient. The reason is that a single value for the rate coefficient is needed in the analysis and 298 K was close to the average daytime high, when photochemistry was the strongest. The values used are given in Table 1 for the OH reaction rate coefficients (Atkinson, 1986; Atkinson & Arey, 2003; Sprengnether et al., 2009) and in Table S1 in the supporting information for the ozone and NO_3 reaction rate coefficients (Aschmann & Atkinson, 2011; Atkinson & Arey, 2003).

3. Results and Discussion

3.1. Importance of Different Hydrocarbon Loss Processes

Evidence for the daytime removal of hydrocarbons is readily observed from the diurnal variations of reactive hydrocarbons as reported previously (Borbon et al., 2013). To illustrate, average diurnal variations of CO and four selected aromatic compounds are presented in Figure 1. The data are averaged in 30 min bins and normalized to a midnight value of one for comparison between different compounds. The figure illustrates that CO and the less reactive hydrocarbons benzene and toluene had a relatively weak dependence on the time of day. On average, there was a modest enhancement in the early afternoon, when the wind speed increased and the wind direction became more consistently from the Southwest, bringing emissions from downtown Los Angeles to the site. The more reactive hydrocarbons (m + p)-xylenes and 1,2,4-trimethylbenzene correlated well with benzene and toluene at night, but were depleted relative to these compounds during the day, because of their more efficient removal by hydroxyl (OH) radicals.

Average nighttime (22:00–6:00 PDT) and daytime (10:00–18:00 PDT) mixing ratios of the measured hydrocarbons are presented in Figure 2a. The highest mixing ratios were observed for the C_2–C_5 alkanes,

Table 1
Emission Ratios (ER ± ΔER) of the Measured Hydrocarbons Versus CO

Compound	k_{OH} at 298 K (cm^3 $molecule^{-1}$ s^{-1})	ER (pptv [ppbv CO]$^{-1}$)	ΔER (pptv [ppbv CO]$^{-1}$)	Background (ppbv)	r^2
Ethane	2.48×10^{-13}	16.5	0.4	1.55 ± 0.09	0.531
Propane	1.09×10^{-12}	13.4	0.3	0.38 ± 0.06	0.615
n-Butane	2.36×10^{-12}	4.94	0.17	0.26 ± 0.03	0.399
i-Butane	2.12×10^{-12}	3.18	0.09	0.135 ± 0.017	0.521
n-Pentane	3.8×10^{-12}	3.40	0.10	0.083 ± 0.017	0.527
i-Pentane	3.6×10^{-12}	8.7	0.4	0[a]	0.665
Hexane	5.2×10^{-12}	1.39	0.07	0	0.243
2-Methylpentane	5.2×10^{-12}	1.43	0.07	0	0.798
3-Methylpentane	5.2×10^{-12}	1.39	0.07	0	0.724
Heptane	6.76×10^{-12}	0.83	0.04	0	0.752
2-Methylhexane	6.69×10^{-12}[b]	0.58	0.03	0	0.807
3-Methylhexane	6.3×10^{-12}[b]	0.58	0.03	0	0.821
n-Octane	8.11×10^{-12}	0.355	0.018	0	0.763
i-Octane	3.34×10^{-12}	1.42	0.06	0[a]	0.842
Nonane	9.7×10^{-12}	0.326	0.017	0	0.816
Decane	1.1×10^{-11}	0.300	0.015	0	0.725
Undecane	1.23×10^{-11}	0.316	0.018	0	0.739
Methylcyclopentane	7.66×10^{-12}[b]	1.34	0.07	0	0.686
Cyclohexane	6.97×10^{-12}	0.53	0.03	0	0.767
Methylcyclohexane	9.64×10^{-12}	0.43	0.02	0	0.660
cis-1,3-Dimethylcyclohexane	$(1.49 \pm 0.08) \times 10^{-11}$[c]	0.114	0.007	0	0.739
trans-1,2-Dimethylcyclohexane	$(1.42 \pm 0.10) \times 10^{-11}$[c]	0.044	0.003	0	0.595
trans-1,3-Dimethylcyclohexane	$(1.45 \pm 0.06) \times 10^{-11}$[c]	0.046	0.003	0	0.828
Ethene	8.52×10^{-12}	11.2	0.6	0	0.924
Propene	2.63×10^{-11}	4.1	0.4	0	0.771
1-Butene	3.14×10^{-11}	0.39	0.03	0	0.853
cis-2-Butene	5.64×10^{-11}	0.28[d]	0.14	0	0.977
trans-2-Butene	6.4×10^{-11}	0.32[d]	0.17	0	0.844
2-Methylpropene	5.14×10^{-11}	0.90[d]	0.15	0	0.775
1,3-Butadiene	6.66×10^{-11}	0.40	0.05	0	0.746
3-Methyl-1-butene	3.18×10^{-11}	0.068	0.006	0	0.741
Isoprene	1.0×10^{-10}	0.52[d]	0.13	0	0.760
Ethyne	8.74×10^{-13}[e]	6.40	0.07	0.059 ± 0.014	0.866
Vinylacetylene	$(3.1 \pm 0.2) \times 10^{-11}$[c]	0.030	0.003	0	0.187
Benzene	1.22×10^{-12}	1.260	0.011	0.028 ± 0.002	0.919
Toluene	5.63×10^{-12}	3.40	0.17	0	0.862
Ethylbenzene	7×10^{-12}	0.61	0.03	0	0.898
(m + p)-Xylenes	1.87×10^{-11}[f]	2.07	0.16	0	0.916
o-Xylene	1.36×10^{-11}	0.77	0.05	0	0.926
Styrene	5.8×10^{-11}	0.36[d]	0.3	0	0.439
n-Propylbenzene	5.8×10^{-12}	0.103	0.006	0	0.890
i-Propylbenzene	6.3×10^{-12}	0.0305	0.0017	0	0.839
1,2,3-Trimethylbenzene	3.27×10^{-11}	0.29	0.03	0	0.731
1,2,4-Trimethylbenzene	3.25×10^{-11}	0.79	0.08	0	0.947
1,3,5-Trimethylbenzene	5.67×10^{-11}	0.39	0.05	0	0.919
o-Ethyltoluene	1.19×10^{-11}	0.123	0.010	0	0.921
(m + p)-Ethyltoluene	1.52×10^{-11}[g]	0.44	0.03	0	0.920

Note. Also given are the background mixing ratios and the linear correlation coefficients derived from the fits. Reaction rate coefficients with OH are taken from Atkinson and Arey (2003) unless noted otherwise.
[a]Set to zero as fit returned negative value. [b]Sprengnether et al., 2009. [c]Rate coefficient derived from the fit of equation (4). [d]Calculated from fit of equation (5) to the nighttime data. [e]Atkinson, 1986. [f]Average of rate coefficients for m- and p-xylene. [g]Average of rate coefficients for m- and p-ethyltoluene.

C_2–C_3 alkenes, ethyne, and the C_6–C_8 aromatics. Most hydrocarbon mixing ratios did not depend strongly on the time of day, except the more reactive alkenes and aromatics, which were significantly reduced in the afternoon. These observations suggest that higher emissions of anthropogenic hydrocarbons during the day and/or the fact that the daytime measurements sampled sources in a wider area with potentially stronger emissions were offset by a deeper mixing layer to result in relatively constant

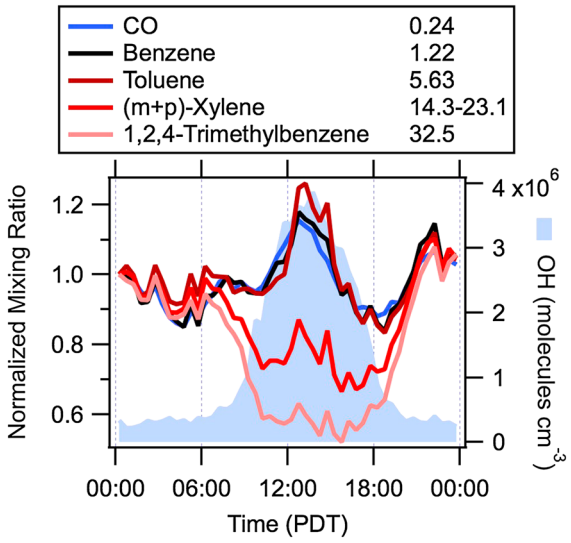

Figure 1. Average diurnal variations of CO and four selected aromatic hydrocarbons. The data are averaged in 30 min bins and normalized to a midnight value of 1 for comparison between the different measurements. The rate coefficients for the reactions with OH are shown in the legend (in units of 10^{-12} cm^3 $molecule^{-1}$ s^{-1}). The blue shaded area indicates the average diurnal variation in measured OH.

mixing ratios throughout day and night. Isoprene was much higher during the afternoon, because its biogenic emissions are light-dependent. Figure 3 shows the ratio between the daytime and nighttime averages as a function of the reaction rate coefficient with the hydroxyl radical (k_{OH}) (Table 1). Isoprene is not included in this graph as its daytime concentrations was much higher. With a few notable exceptions, the decrease in afternoon mixing ratios can be described by a single exponential function of k_{OH}, indicated by the gray curve in Figure 3. In other words, OH chemistry during the day was the dominant loss mechanism for most hydrocarbons. Surface concentrations of reactive hydrocarbons can also decrease as a result of vertical mixing during the day with air masses aloft that have lower concentrations. However, more reactive compounds have typically stronger vertical gradients, so OH chemistry also plays a role in these processes. Two groups of compounds did not follow this general trend. Three alkenes (cis-2-butene, trans-2-butene, and 2-methylpropene) and styrene are very reactive with ozone and NO_3, and their nighttime removal cannot be ignored as will be shown below. Because the nighttime removal is significant, the daytime versus nighttime ratios of these compounds are higher than expected from OH chemistry only. The same is true for the three measured monoterpenes (α- and β-pinene and limonene). These compounds also have higher biogenic emissions during the day when temperatures are higher. It is also notable that ethane is lower during the day than at night. Ethane is primarily released from natural gas pipeline and production leaks in the basin (Peischl et al., 2013). A more constant emission flux in time combined with dilution in an expanding boundary layer during the day may explain this observation.

The main oxidants OH, ozone, and NO_3 were all measured at the site (Figures 4a–4c). Measurements of OH and ozone were made in situ (Griffith et al., 2016), whereas NO_3 was measured by long-path DOAS between the top of the Millikan library and retroreflectors at four different levels in the San Gabriel mountains (Tsai et al., 2014). The data showed a strong vertical gradient in NO_3 increasing with height. Here we use the NO_3 data from the lowest light path, which likely overestimate NO_3 at the surface. The hydrocarbon loss rates versus different oxidants are calculated as the products of the oxidant concentrations times the rate coefficients for their reactions with the different hydrocarbons (Figures 4d–4i). For alkanes and aromatics, loss rates were dominated by OH reactions during the day. For most alkenes, the removal was dominated by OH, but reactions with ozone were not negligible. For some alkenes, the removal was not dominated by OH, but also determined by ozone during the day, and by NO_3 and/or ozone at night. Loss rates averaged over the whole data set for all measured hydrocarbons against OH, ozone and NO_3 are compared in Figure 2b, again illustrating the dominant role of OH for all hydrocarbons except the alkenes, styrene, and terpenes. It should again be noted that the NO_3 loss rates likely overestimate the values at the surface due to the fact that NO_3 was measured by LP-DOAS and biased by higher NO_3 aloft. On the other hand, OH and ozone also have some dependence on height. Nighttime ozone increased with height (Tsai et al., 2014) and early morning OH may have decreased with height as HONO, one of its precursors, is formed at the surface (Young et al., 2012). The loss rates of hydrocarbons at the surface are therefore not equal to the average loss rates throughout the daytime and nighttime boundary layers, but the relative importance of different loss rates will not be much different from those shown in Figure 2b.

Not included in this analysis is removal by chlorine (Cl) radicals, which were not measured at the site. A previous analysis of Cl_2 and $ClNO_2$ measurements made from the research vessel Atlantis during CalNex suggested that Cl radicals can provide an additional loss process for alkanes in the morning (Riedel et al., 2012). The effects of chlorine chemistry have been studied previously using hydrocarbon ratios (Gilman et al., 2010), but no similar evidence is found from this data set (Figure S3). We conclude that hydrocarbon removal by Cl atoms at the ground site in Pasadena was a minor loss process and have omitted it from the analysis. Finally, photolysis is not an important loss process for the hydrocarbon compounds included in this analysis.

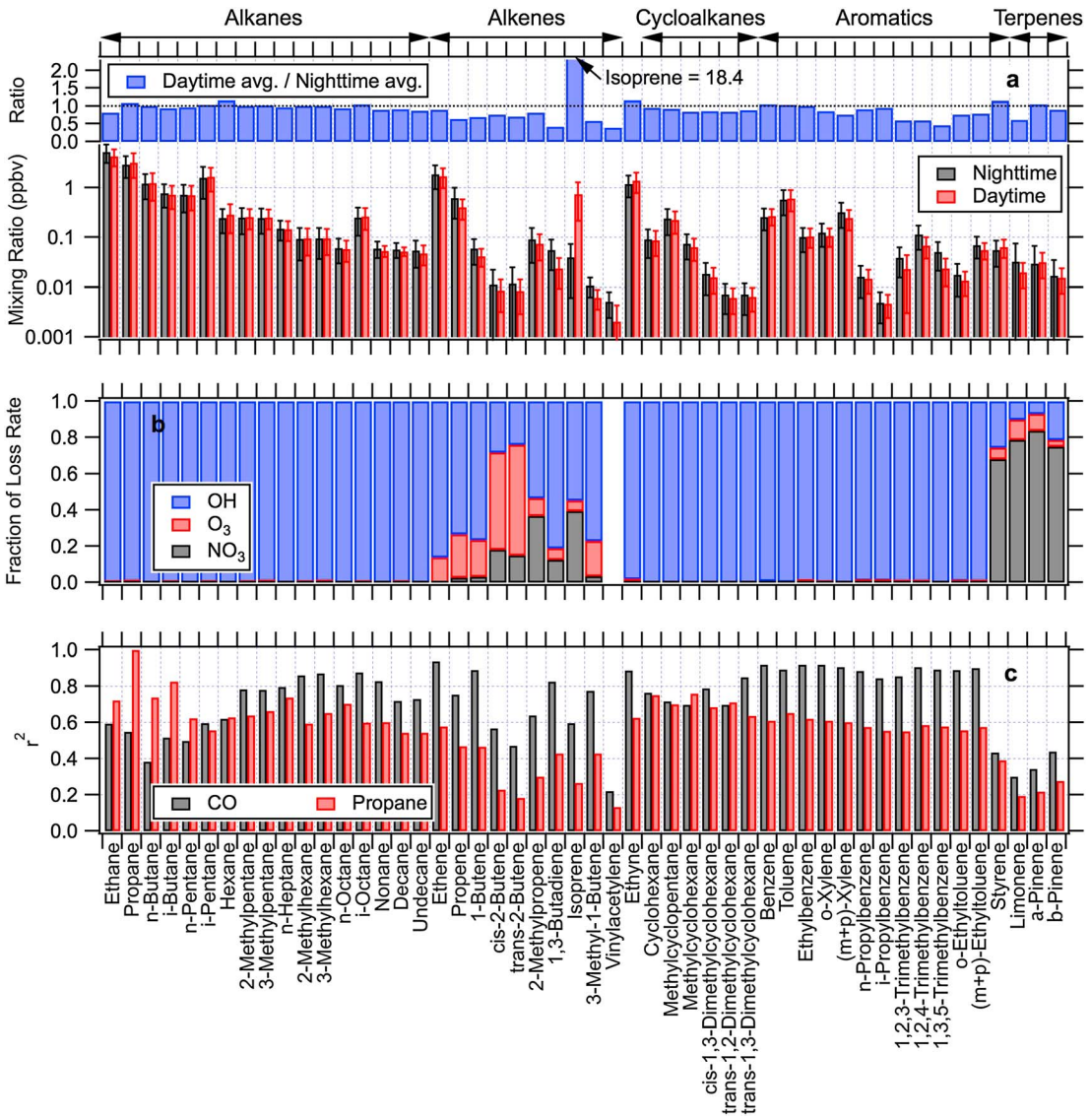

Figure 2. (a) Average daytime (10:00–18:00 PDT) and nighttime (22:00–6:00 PDT) mixing ratios for the measured hydrocarbons, with the error bars indicating the standard deviations. The ratio between daytime and nighttime averages are shown in blue. The dotted line shows a ratio of 1. (b) Relative importance of campaign-average in situ loss rates for different hydrocarbons versus OH, ozone, and NO_3. Reaction rate coefficients for vinylacetylene could not be found. (c) Linear correlation coefficients between nighttime data for the measured hydrocarbons with CO and propane, respectively.

The focus on diurnal variations and daily averages in this section disregards the day-to-day variability due to weather conditions and other factors. Photochemical activity and ozone chemistry in the basin were the strongest during two warm periods from 2 to 9 and 13 to 15 June 2010 and were much less pronounced during a cooler period from 23 to 27 May 2010 that had some precipitation. Differences in hydrocarbon emissions and oxidation between weekends and weekdays during CalNex have been studied (Warneke et al., 2013). In summary, photochemical removal of hydrocarbons was more efficient on weekends when NO_x emissions from trucks were reduced (Kim et al., 2016), but the composition of hydrocarbon emissions did not change between weekends and weekdays.

3.2. Determination of Hydrocarbon Emission Ratios

We have previously determined emission ratios of hydrocarbons versus CO from this and other data sets using nighttime data, based on the assumption that removal of most hydrocarbons is inefficient at night (Borbon et al., 2013; Warneke et al., 2007). The results in Figures 2–4 call into question whether this

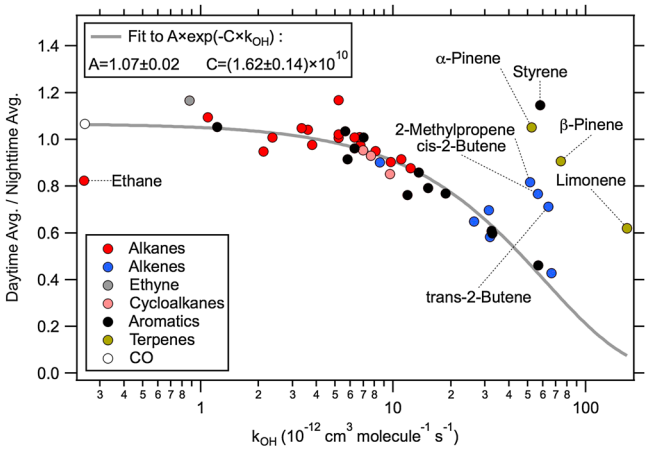

Figure 3. Ratio between the average daytime (10:00–18:00 PDT) and nighttime (22:00–6:00 PDT) mixing ratios of different hydrocarbons and CO as a function of the reaction rate coefficient with hydroxyl radicals. The gray curve shows a fit of a single exponential function to the data. Not included is isoprene, which was much higher during the day, because its emissions are light-dependent.

method accurately determines emissions of reactive alkenes. Scatterplots of hydrocarbons versus CO generally show a high degree of correlation at night, but the correlation is lost during the day for those species that are efficiently removed by OH. Several examples are shown in Figure S4 in the supporting information. Figure 2c summarizes the linear correlation coefficients for the measured hydrocarbons versus CO for the nighttime data (22:00–6:00 PDT). Nighttime correlations were strongest for the aromatic hydrocarbons, ethene, propene, and the C_6–C_9 alkanes. Nighttime correlations were notably weaker for the reactive alkenes and styrene, that is, the same species that show significant nighttime removal in Figure 2b. A different illustration of this observation is given in Figure S5, which shows the nighttime correlations as a function of the reaction rate coefficients with ozone and NO_3. Nighttime correlations were also weaker for the C_2–C_5 alkanes, which have different sources than CO related to fossil fuel production and distribution, as well as hydrocarbon seeps in the basin (Peischl et al., 2013). As a result, the C_2–C_5 alkanes correlated more strongly with propane as shown in Figure 2c. Nighttime correlations were weak for the terpenes, which have biogenic sources that are not related to those of CO; terpene emission ratios versus CO are not meaningful quantities. Isoprene showed stronger correlation with CO at night than the terpenes and in the same range as observed for other reactive alkenes. These observations may be indicative of an anthropogenic source of isoprene as reported previously (Borbon et al., 2001).

In our previous work, we have used both CO and ethyne as more inert tracers for urban emissions (Borbon et al., 2013; de Gouw et al., 2005; Warneke et al., 2007). In the current data set, most VOCs correlated more strongly at night with CO than with ethyne (Figure S6). We will therefore focus on emission ratios versus CO in this paper. One complication is that CO has a nonzero regional background that must be considered

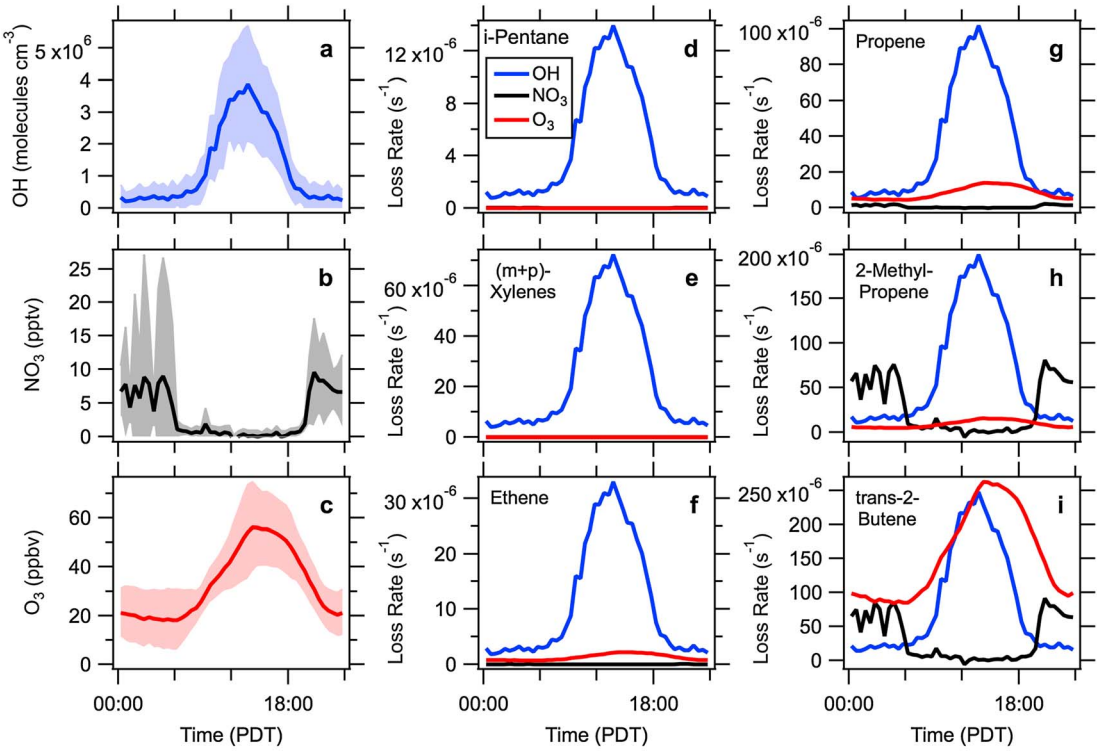

Figure 4. Average diurnal variations of (a) OH, (b) NO_3, and (c) O_3, with the solid curves representing the average in 30 min bins and the shaded areas representing the 1σ variability. (d–i) The calculated loss rates for six selected hydrocarbons versus OH in blue, NO_3 in black, and O_3 in red.

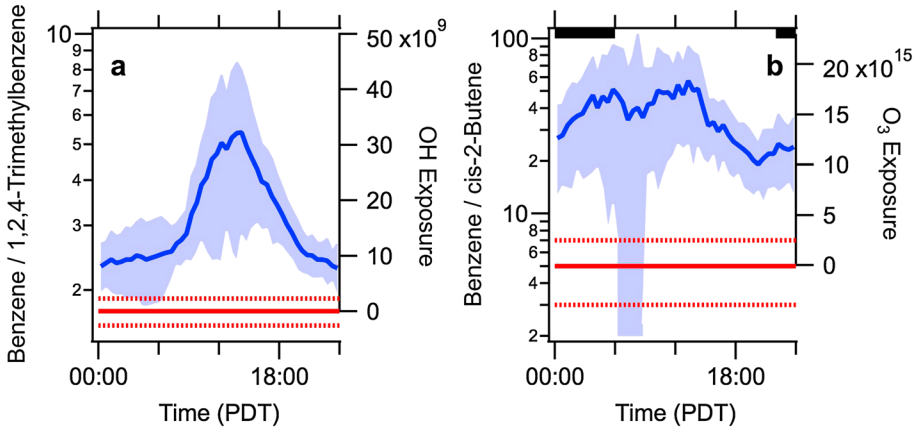

Figure 5. The use of measured hydrocarbons to quantify exposure to OH radicals and to ozone and NO_3 at night. (a) The diurnal variation in benzene/1,2,4-trimethylbenzene with the blue curve representing the average in 30 min bins and the blue shaded area representing the 1σ variability. (b) The diurnal variation in benzene/cis-2-butene. The right axes in both panels show the conversion of these hydrocarbon ratios into OH and ozone exposures, respectively (in units of molecules cm^{-3} s). For ozone exposure, only nighttime (22:00–6:00 PDT) values are used, indicated by the solid black bars at the top axis of Figure 5b. The solid and dashed red lines show the emission ratios and their uncertainties.

in this analysis. A value of 115 ± 10 ppbv is determined here from the intercepts of reactive hydrocarbons versus CO as discussed in Figure S7 in the supporting information. This CO background agrees within the uncertainties with the weekday and weekend backgrounds reported previously for the CalNex period (Pollack et al., 2012). Photochemical formation of CO itself is ignored and was likely very small relative to background concentration as evidenced by the strong correlations between CO and less reactive hydrocarbons, and as expected from model calculations (Griffin et al., 2007).

Several analyses of this data set have previously made use of hydrocarbon ratios to parameterize the exposure of sampled emissions to OH radicals (Borbon et al., 2013; Ensberg et al., 2014; Hayes et al., 2013; Zhao et al., 2014). A similar concept was used to quantify the aging of particle-phase hydrocarbons at the site (Chan et al., 2013). Figure 5a shows the average diurnal variation in the ratio of benzene over 1,2,4-trimethylbenzene. Both aromatic compounds had negligible nighttime removal and the ratio increased significantly during the day, when 1,2,4-trimethylbenzene was removed more efficiently than benzene. Similarly, ratios involving reactive alkenes may be useful to describe the effects of nighttime chemistry. For example, the ratio of benzene versus cis-2-butene had a significantly different diurnal variation (Figure 5b). There was a daytime peak around noon: cis-2-butene is also highly reactive with OH ($k_{OH} = 56.4 \times 10^{-12}$ cm^3 $molecule^{-1}$ s^{-1}). An additional rise in the ratio occurred throughout the night ending at sunrise on many days. This second maximum is attributed here to the combined removal by ozone and NO_3 at night.

The time-integrated exposure of emissions to OH (OH exposure or [OH]Δt) can be calculated from the ratio of benzene (Ben) over 1,2,4-trimethylbenzene (124TMB) as in previous analyses (Borbon et al., 2013; Ensberg et al., 2014; Hayes et al., 2013). As a function of time after emission, this ratio can be written as

$$\mathrm{Ben}/124\mathrm{TMB} = \mathrm{ER}_{\mathrm{Ben}/124\mathrm{TMB}} \times e^{\left(k_{124\mathrm{TMB}+\mathrm{OH}} - k_{\mathrm{Ben}+\mathrm{OH}}\right)[\mathrm{OH}]\Delta t} \quad (1)$$

where $\mathrm{ER}_{\mathrm{Ben}/124\mathrm{TMB}}$ is the emission ratio that is assumed to be constant across the basin and $k_{124\mathrm{TMB}+\mathrm{OH}}$ and $k_{\mathrm{Ben}+\mathrm{OH}}$ are the rate coefficients for the reaction with OH. This equation can be rearranged to solve for the OH exposure:

$$[\mathrm{OH}]\Delta t = \frac{1}{k_{124\mathrm{TMB}+\mathrm{OH}} - k_{\mathrm{Ben}+\mathrm{OH}}} \times \left(\ln\left(\frac{\mathrm{Ben}}{124\mathrm{TMB}}\right) - \ln\left(\mathrm{ER}_{\mathrm{Ben}/124\mathrm{TMB}}\right) \right) \quad (2)$$

The OH exposure depends linearly on the logarithm of the measured ratio between the two hydrocarbons and equals zero when the measured ratio is equal to the emission ratio. The emission ratio is not known a priori and is estimated here to be 1.75 ± 0.15 ppbv $ppbv^{-1}$ (solid and dotted red lines in Figure 5a) from air masses with a low degree of photochemical processing. These air masses were identified using the

time series and diurnal variation of measured benzene/1,2,4-trimethylbenzene ratios and using scatterplots of benzene versus 1,2,4-trimethylbenzene; further details are shown in Figure S8 in the supporting information. The estimated emission ratio can be compared with results from three urban studies (U.S. East Coast, Beijing, Paris) (Borbon et al., 2013; Warneke et al., 2007; Yuan et al., 2012), a tunnel study (Gentner et al., 2013) and two dynamometer studies of motor vehicle emissions (May et al., 2014; Schauer et al., 2002), which give a range in the benzene/1,2,4-trimethylbenzene ratio from 1.4 to 3.4 ppbv ppbv^{-1} with an average of 2.6 ± 0.8 ppbv ppbv^{-1}. This emission ratio agrees within the error bars with the presently reported value of 1.75 ± 0.15 ppbv ppbv^{-1}. We prefer the lower value as many air masses had measured benzene/1,2,4-trimethylbenzene ratios that were lower than 2.6 and indeed were less aged judging from other hydrocarbon measurements.

Using this emission ratio, the OH exposure is calculated and shown on the right axis of Figure 5a. The average daytime maximum is ~30×10^9 molecules cm^{-3} s. Using the average daytime maximum OH concentration of ~4×10^6 molecules cm^{-3} (Figure 4a), this corresponds to a processing time of ~2 h, which is similar to the time for emissions to be transported from the main sources in the Los Angeles basin to the measurement site in Pasadena. Of course, the in situ OH may not be fully representative of the OH concentrations that the sampled air masses encountered since the time of emission. Therefore, arguments such as these are semi-quantitative at best but do support the plausibility of the OH exposure in Figure 5a. The uncertainty in the assumed emission ratio results in a bias in the OH exposure according to equation (2). Estimates of OH exposure from other hydrocarbon pairs are quantified in the supporting information and largely agree with the values calculated from benzene versus 1,2,4-trimethylbenzene using the assumed emission ratio described above (Figure S9).

By analogy with equation (2), the ozone exposure at night can be calculated from the measured ratio of benzene over cis-2-butene (c2But). Cis-2-butene is used here as it reacts efficiently with ozone, and the nighttime losses to ozone are higher than those to NO_3 (Figure 2b and Table S1):

$$[O_3]\Delta t = \frac{1}{k_{c2But+O3} - k_{Ben+O3}} \times \left(\ln\left(\frac{Ben}{c2But}\right) - \ln\left(ER_{Ben/c2But}\right)\right) \quad (3)$$

where $ER_{Ben/c2But}$ is the emission ratio between benzene and cis-2-butene and $k_{c2But + O3}$ and $k_{Ben + O3}$ are the rate coefficients for the reaction with ozone. This is only an approximate measure of nighttime processing, because reactions with NO_3 cannot be ignored for several compounds. These limitations will be discussed further below. The emission ratio $ER_{Ben/c2But}$ is estimated as 5 ± 2 (Figure S10) and indicated by the red line in Figure 5b. This emission ratio is much more uncertain, as it is determined by a few samples only; the extent of chemical removal of cis-2-butene was extensive at most times during the mission. Again, the number can be compared with results from the urban, tunnel, and dynamometer studies (Borbon et al., 2013; Gentner et al., 2013; May et al., 2014; Schauer et al., 2002; Warneke et al., 2007; Yuan et al., 2012), which give a range in benzene/cis-2-butene ratios of 9–13 ppbv ppbv^{-1} with an average of 10 ± 2 ppbv ppbv^{-1}. This ratio is higher than the value used here, but we prefer the lower value as many air masses had measured benzene/cis-2-butene ratios that were lower than 10 and indeed those air masses appeared to be less aged judging from the combined hydrocarbon measurements.

The ozone exposure, calculated using equation (3), is shown on the right axis of Figure 5b; only nighttime values (22:00–6:00 PDT) for the ozone exposure are used below, as daytime benzene/cis-2-butene ratios are also affected by OH chemistry. Nighttime ozone exposures ranged from (10–20) $\times 10^{15}$ molecules cm^{-3} s. Using an average nighttime ozone mixing ratio of 20 ppbv, this corresponds to a processing time of 5–10 h, suggesting that the aging of hydrocarbons by ozone and NO_3 progressed gradually during the night.

The ratios of various hydrocarbons over CO are shown as a function of OH and nighttime ozone exposure in Figure 6. In the case of OH exposure, all data are included in the analysis, whereas only nighttime data are included for ozone exposure. Ratios of 1,3,5-trimethylbenzene and propene over CO depend strongly on OH exposure but only weakly on the nighttime ozone exposure as expected from the reaction rate coefficients for these compounds. The ratios of 2-methylpropene and trans-2-butene over CO do depend on OH exposure, but the data contain much more variability than is described by a single exponential function. We attribute this to the fact that these compounds are efficiently lost by OH but also by ozone and NO_3 (Figures 2–4). In contrast with 1,3,5-trimethylbenzene and propene, the ratios of 2-methylpropene and

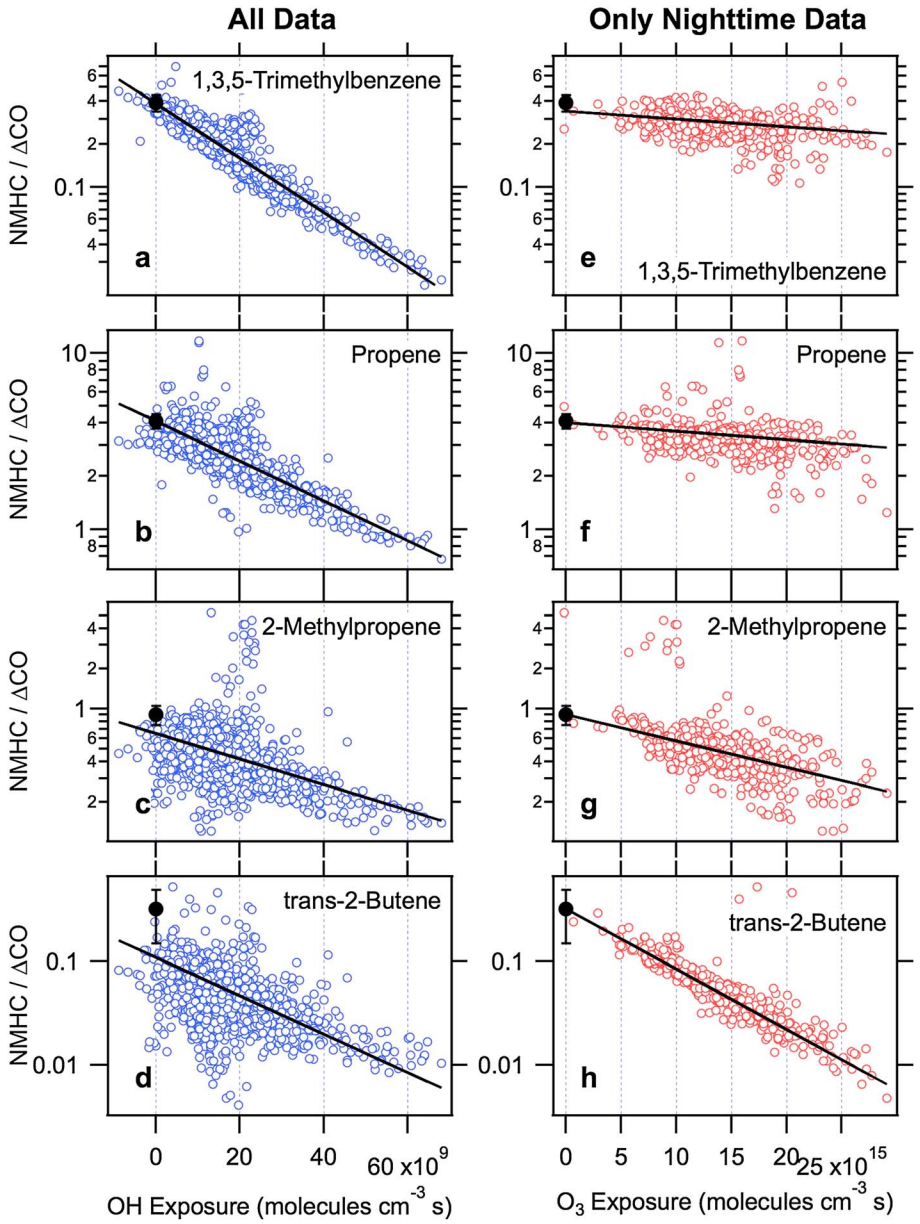

Figure 6. (a–h) Ratios of various hydrocarbons versus CO (in pptv [ppbv CO]$^{-1}$) as a function of OH exposure on the left (blue) and as a function of nighttime ozone exposure on the right (red). The black lines in Figures 6a–6d represent fit results of equation (4) to all the measurement data. The black lines in Figures 6e–6h represent fit results of equation (5) to the nighttime data only. The black circles and error bars represent the emissions ratios derived from the fits (using equation (4) for 1,3,5-trimethylbenzene and propene and using equation (5) for 2-methylpropene and trans-2-butene).

trans-2-butene over CO depend more strongly on the nighttime ozone exposure. The range in these ratios at night is as high as it is for the data set as a whole.

Analyses as in Figure 6 are useful to determine emission ratios for all hydrocarbons, by extrapolating the ratios of hydrocarbons over CO to a zero OH exposure or zero nighttime ozone exposure. The hydrocarbon data can be described as a function of OH exposure as

$$\mathrm{HC} = \mathrm{background} + \mathrm{ER_{HC}} \times \Delta\mathrm{CO} \times e^{-(k_{\mathrm{HC+OH}} - k_{\mathrm{CO+OH}})[\mathrm{OH}]\Delta t} \quad (4)$$

and as a function of nighttime ozone exposure as

$$\mathrm{HC} = \mathrm{background} + \mathrm{ER_{HC}} \times \Delta\mathrm{CO} \times e^{-k_{\mathrm{HC+O3}}[\mathrm{O_3}]\Delta t.} \quad (5)$$

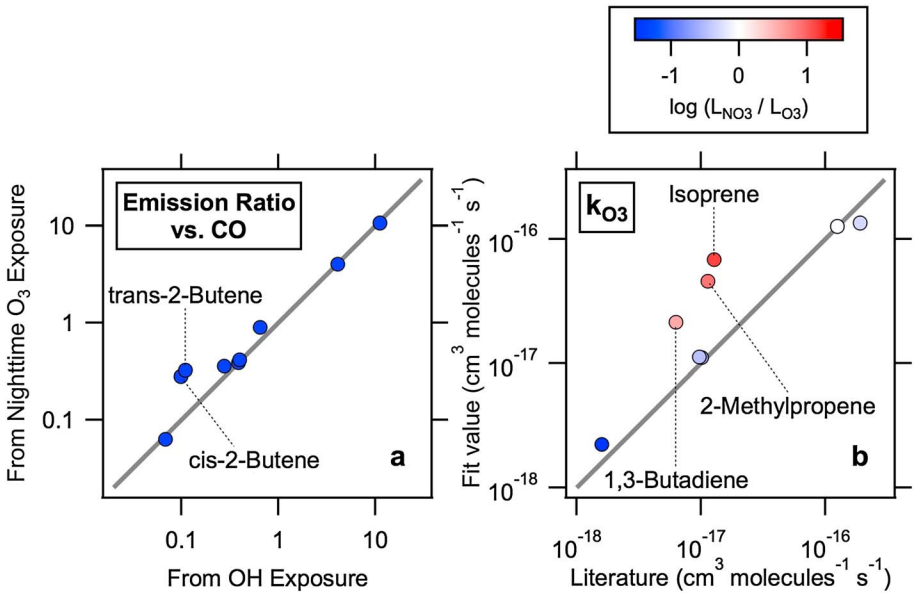

Figure 7. (a) The emission ratios for alkenes determined from the fits versus nighttime ozone exposure compared with the results from the fits versus OH exposure (in pptv [ppbv CO]$^{-1}$). (b) The apparent nighttime removal rate for alkenes as a function of their ozone reaction rate coefficients. The data points are color-coded by the ratio between the loss rates versus NO_3 and ozone, calculated using the respective rate coefficients and average NO_3 and ozone mixing ratios of 5 pptv and 20 ppbv, respectively. The gray lines show the 1:1 relationships.

The addition of a background in these functions is required for the less reactive hydrocarbons ($k_{OH} < 5 \times 10^{-12}$ cm^3 molecule^{-1} s^{-1}; Figure S7). Emission ratios were calculated for all hydrocarbons using a fit of equation (4) to the data. The black lines in Figures 6a–6d show results for four selected compounds; resulting emission ratios for all species are shown in Table 1 (except for a few alkenes, where the listed value is derived from the nighttime data using equation (5) as discussed below). For the less reactive hydrocarbons ($k_{OH} < 5 \times 10^{-12}$ cm^3 molecule^{-1} s^{-1}), the reaction rate coefficient was fixed at its literature value and the emission ratio ER_{HC} and background were used as free variables in the fit. For the more reactive hydrocarbons, the background was fixed at zero and the emission ratio and reaction rate coefficient were used as free variables. The emission ratios from the fits are compared for all hydrocarbons except alkenes with the emission ratios from (Borbon et al., 2013) in Figure S11. The latter values were derived from linear fits to the nighttime data only and agree well with the present results, because the compounds included have negligible nighttime removal. Figure S11 also shows a comparison between the reaction rate coefficients from the fits and those from the literature.

The random errors in the emission ratios in Table 1 were estimated from three factors:

1. The random error from the fit of equations (4) and (5) to the data. These errors tend to dominate for the least reactive hydrocarbons and compounds that do not correlate with CO as strongly.
2. The errors in the assumed emission ratios $ER_{Ben/124TMB}$ and $ER_{Ben/c2But}$ that define zero OH and ozone exposure. These errors were calculated by repeating the above calculation with $ER_{Ben/124TMB}$ (1.75 ± 0.15) and $ER_{Ben/c2But}$ (5 ± 2) at the upper and lower ends of their estimated uncertainty ranges to quantify the difference with the central estimate. These errors tend to dominate for the most reactive hydrocarbons that depend strongly on OH and ozone exposure, in which case a bias in the exposure can lead to a substantially different emission ratio.
3. The error in the CO background (115 ± 10 ppbv). This error was calculated by repeating the above calculation with the CO background at the upper and lower ends of its uncertainty range to quantify the difference with the central estimate. This error tends to dominate for all but the most and least reactive compounds.

In principle, fitting equation (4) to all data and fitting equation (5) to the nighttime data only should give the same values for the *background* and emission ratio ER_{HC}. However, in cases where nighttime

chemistry is efficient, equation (4) does not accurately describe the observed variability and equation (5) gives more accurate results for the emission ratio. This can be illustrated using the data for trans-2-butene. At zero OH exposure, there is a range of almost an order of magnitude in the ratio of trans-2-butene over CO (Figure 6d). Fitting equation (4) to the data returns a value that is in the middle of that range. However, Figure 6h shows that much of the variability at night can be explained by the ozone exposure. Extrapolation of the trans-2-butene/CO ratio to zero nighttime ozone exposure results in an emission ratio that is a factor of ~3 higher than the emission ratio obtained from extrapolating to zero OH exposure. Data for 2-methylpropene and trans-2-butene show a clearer dependence on OH exposure if only daytime data are included in the graphs (Figure S12). However, the emission ratio for trans-2-butene versus CO obtained from extrapolating to zero OH exposure still underestimates the value obtained from the analysis of nighttime data.

Emission ratios were calculated for all alkenes using a fit of equation (5) to the nighttime data only. Results for four selected species are shown by the black lines in Figures 6e–6h. Figure 7a compares the emission ratios for the alkenes from the fits of equation (5) to the nighttime data versus those from the fits of equation (4) to the whole data set. Most species agree well, but for cis-2-butene and trans-2-butene the emission ratios calculated from the fits versus nighttime exposure are a factor of ~3 higher. The emission ratios in Table 1 include these updated emission ratios and these values supersede our previously reported numbers (Borbon et al., 2013). Figure 7b compares the reaction rate coefficients from the fits of equation (5) to the data with the ozone reaction rate coefficients from the literature. The values agree closely except for 1,3-butadiene, 2-methyl propene, and isoprene, which are exactly the species that are more efficiently lost through reaction with NO_3 (Figure 2). To illustrate this point further, the data in Figure 7b are color-coded by the calculated loss rates of these alkenes at average NO_3 and ozone mixing ratios of 5 pptv and 20 ppbv, respectively. When the loss is dominated by ozone reactions (blue points), the data fall along the 1:1 line in Figure 7b. In contrast, when the loss by NO_3 reactions is faster (red points), the data fall above the 1:1 line. An alternative analysis based on nighttime NO_3 exposures calculated from benzene versus 2-methylpropene ratios is likely possible, but this has not been attempted for the present study.

3.3. Evaluation of Analysis Methods Using WRF-Chem Model

In the atmosphere, emissions from specific sources are diluted, transported, mixed with less aged emissions from other sources, and removed by different chemical processes. The question arises if the methods deployed in the previous sections account for these processes and allow the composition of emissions to be determined accurately. To evaluate the methods used here to determine emissions, we repeated the same analysis as above for output from the WRF-Chem model. Following the same methods, emission ratios were calculated for the various, lumped hydrocarbon species in the model using only the model output at the Pasadena site. Of course, the modeled emissions are known and can then be compared with the emissions derived using the model output by the methods developed here.

The same analyses as presented above in Figures 1–7 were repeated for the WRF-Chem model output for Pasadena for the lumped compounds ETH (ethane), HC3 (alkanes, alkynes, and alcohols with $k_{OH} < 3.4 \times 10^{-12}$), HC5 (alkanes, alkynes, and alcohols with $3.4 \times 10^{-12} < k_{OH} < 6.8 \times 10^{-12}$), HC8 (alkanes, alkynes, and alcohols with $k_{OH} > 6.8 \times 10^{-12}$), ETE (ethene), OLT (terminal olefins), OLI (internal olefins), TOL (toluene and less reactive aromatics), and XYL (xylene and more reactive aromatics) (Stockwell et al., 1997). The following results are shown in the supporting information in detail:

1. Average diurnal variations for modeled hydrocarbons in Pasadena show that the more reactive compounds are removed during the day relative to the less reactive compounds (Figure S13).
2. Comparison of the daytime and nighttime averages (Figure S14) show that the removal of most hydrocarbons is governed by OH, except for the OLI compounds, which show less removal during the day relative to what is expected from OH chemistry (Figure S15). One difference with the measurements is that the modeled daytime averages are lower than the nighttime averages even for the less reactive hydrocarbons. On average, the modeled carbon monoxide did not show a decrease during the day relative to nighttime (Kim et al., 2016), so the reduction in less reactive hydrocarbons during the day must be caused by the representation of emissions in the NEI-2011 rather than the model description of boundary layer dynamics.

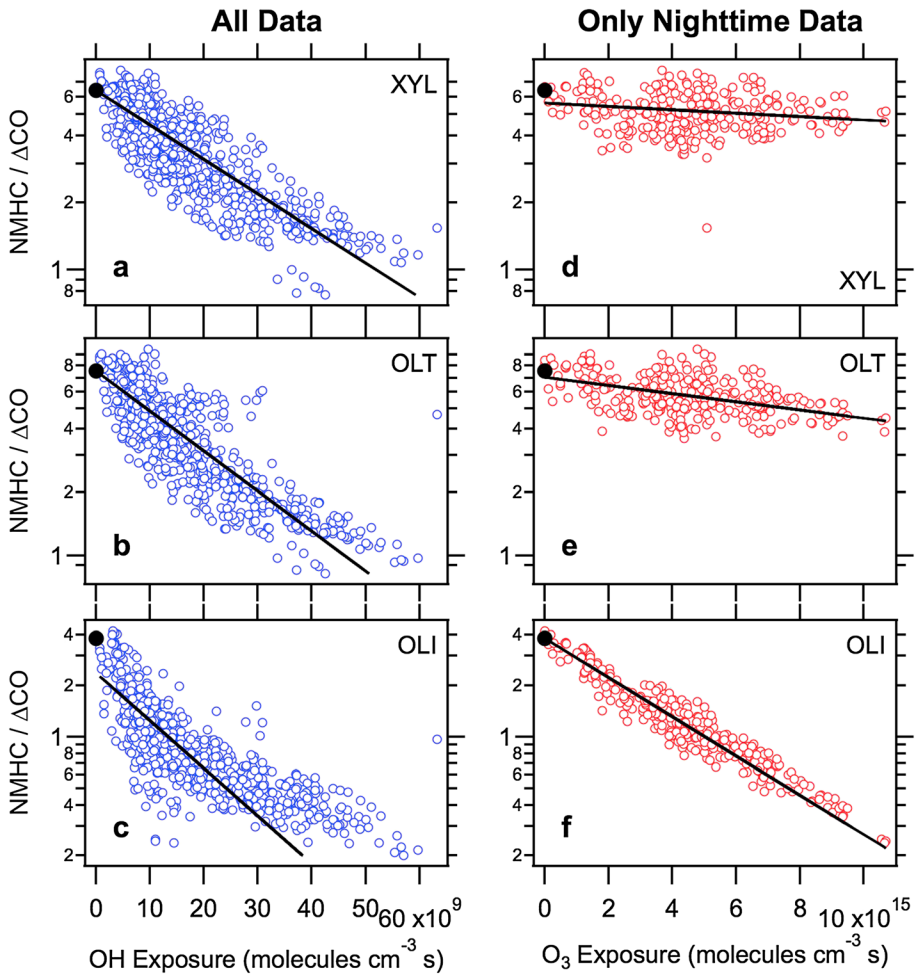

Figure 8. Ratios of various modeled hydrocarbons versus CO (in pptv [ppbv CO]$^{-1}$) as a function of OH exposure on the left (blue) and as a function of nighttime ozone exposure on the right (red). The black lines represent fit results of equations (4) and (5) to the model data. The black circles represent the emissions ratios derived from the fits (using equation (4) for XYL and OLT and using equation (5) for OLI).

3. Based on the modeled OH, ozone, and NO_3, the calculated hydrocarbon loss rates show similar diurnal variations (Figure S16) and relative importance averaged over the entire mission (Figure S14) as the measurements.
4. Scatterplots of modeled hydrocarbons versus CO show a stratification by the time of day, which is stronger for compounds that react more efficiently with OH (Figure S17). For the OLI compounds, there is a very weak correlation with CO at night, because of the efficient nighttime removal of OLI. One notable difference between the measurements and model is that the measured hydrocarbons and CO are more tightly correlated than the modeled hydrocarbons and CO (Figure S14). Evidently, the sources of hydrocarbons and CO are not as tightly coupled in the model as they are in the real atmosphere. The stratification by time of day in the scatterplots of ETH and HC3 versus CO again shows that modeled emission ratios must depend on the time of day in the model. A strong stratification by time of day for less reactive hydrocarbons was not observed in the measurements (Figure S4).
5. The hydrocarbon ratios HC3/XYL and HC3/OLI can be used to quantify OH exposure and nighttime ozone exposure, respectively. Similar to the measurements, the HC3/XYL ratios show a daytime peak due to OH chemistry, and the HC3/OLI ratios show an additional nighttime peak due to nighttime removal of OLI by ozone and NO_3 (Figure S18). The values of OH exposure derived from the model output and estimated emission ratios (Figure S19) are close to those calculated from the measurements. The values for ozone exposure derived from the model output are somewhat lower than those calculated from the measurements.

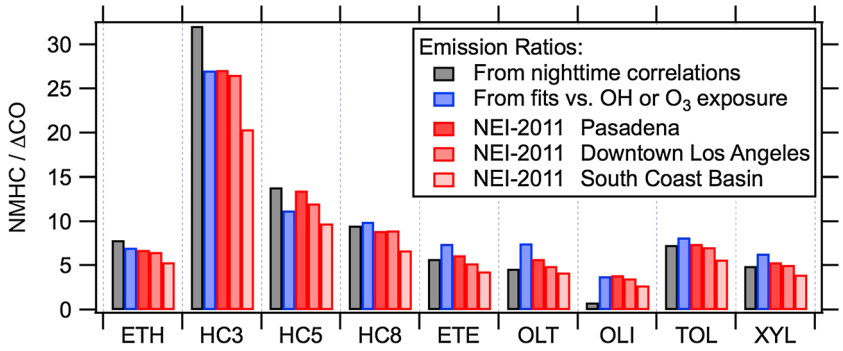

Figure 9. Comparison of emission ratios (in pptv [ppbv CO]$^{-1}$) determined from the WRF-Chem model output for Pasadena using the same methods used to analyze the measurement data with the emission ratios from NEI-2011 averaged over three different domains.

Emission ratios can now be estimated from the model output, analogously to the analysis of the measurement data shown in Figure 6. Figure 8 shows the dependence of several different hydrocarbon species in the model as a function of OH exposure and nighttime ozone exposure. The XYL and OLT compounds depend strongly on OH exposure and only weakly on nighttime ozone exposure, similarly to what was found for 1,3,5-trimethylbenzene and propene in the measurement data. The OLI compounds depend on OH exposure, but more strongly on nighttime exposure, similarly to what was seen for trans-2-butene in the measurements. Emission ratios are calculated by fitting equations (4) and (5) to the modeled data versus OH exposure and nighttime ozone exposure, respectively. As was the case for the measurements, the model output for OLI shows significant variability at zero OH exposure, and the emission ratio calculated from a fit of equation (4) gives a value somewhere in the middle of that range (Figure 8c). A higher emission ratio for OLI was obtained from the fit of equation (5) to the nighttime data (Figure 8f).

Emission ratios of the hydrocarbons in the model versus CO, calculated from the fits of equations (4) and (5) to the model output, are presented in Figure 9 and compared with the ratios between the hydrocarbon and CO emissions from the NEI-2011 inventory. Modeled emission ratios were extracted in three different domains (Pasadena, downtown Los Angeles, and the entire South Coast Basin; Figure S20). While the emission ratios for Pasadena and downtown Los Angeles were very similar, the emission ratios for the South Coast Basin were ~23% lower on average. On average, the emission ratios calculated from the WRF-Chem model output at Pasadena agree with the NEI-2011 data for the Pasadena domain (Figure S21) and are also representative of the downtown Los Angeles domain. Importantly, the agreement between the emissions ratios in Figure 9 holds true for less and more reactive hydrocarbons, which provides evidence that the analysis does allow the effects of emissions and chemistry to be separated. Also added to Figure 9 are emission ratios derived from nighttime correlations of the model output, that is, the method used previously to determine emission ratios (Borbon et al., 2013). These latter emission ratios are on average 12% higher than the NEI-2011 data, except for the OLI compounds (Figure S21), which have underestimated emissions due to the importance of nighttime removal.

An analysis of the model output provided evidence that emissions of hydrocarbons and CO have different diurnal variations (Figures S15 and S17). Notably, daytime versus nighttime ratios were different for hydrocarbons and for CO in the model output. Indeed, it was found that the ratios between hydrocarbon and CO emissions in the model vary strongly by the time of day. As an example, Figure S22 shows the diurnal variations in the modeled emissions of CO and TOL for the Pasadena domain. The CO emissions show a larger enhancement during the day relative to the nighttime and also show a stronger increase with time in the early morning than the TOL emissions. As a result, the emission ratio of TOL versus CO depends on the time of day. The same was true for the other hydrocarbons and in each of the three domains in Figure S20. The diurnal variation in modeled emission ratios is actually stronger than the daytime versus nighttime stratification in the measurements (Figure S17): air masses at night contain hydrocarbons from a range of locations and emission times, which averages their composition.

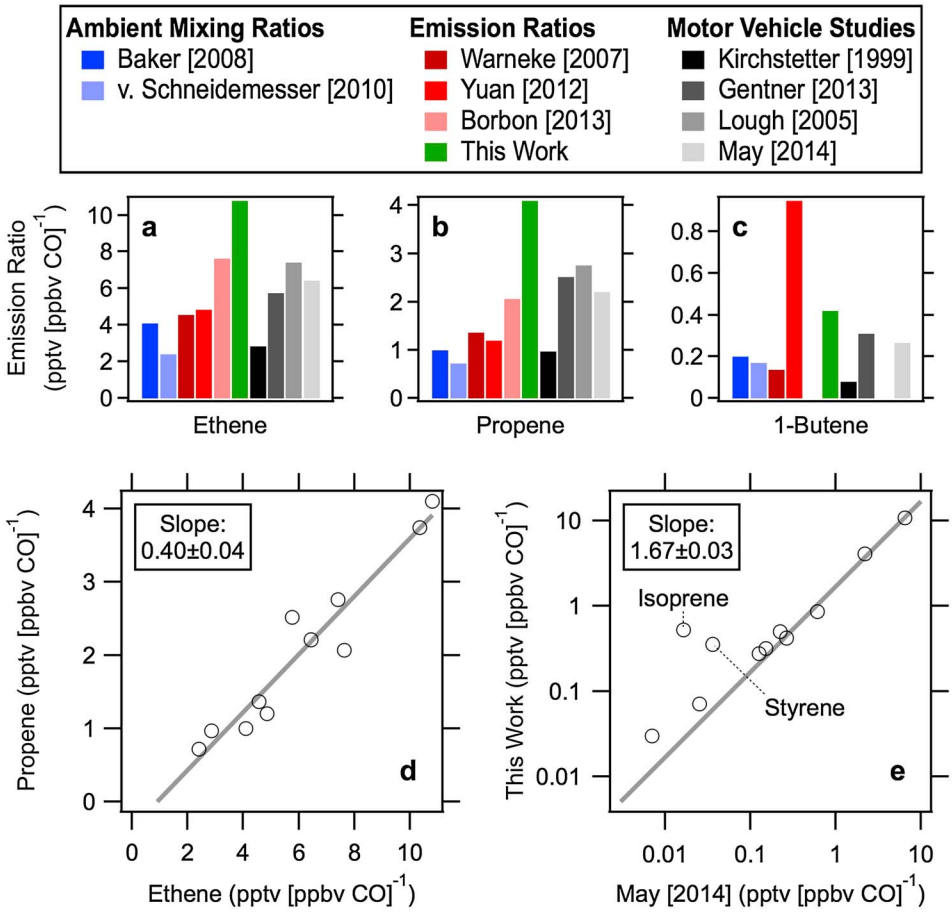

Figure 10. (a–c) Comparison between alkene emission ratios determined in this work and results from the literature. (d) Scatterplots of propene versus ethene emission ratios from the above studies. (e) Comparison between the emission ratios determined in this work and those from a detailed dynamometer study of motor vehicle emissions (May et al., 2014).

The above analysis of WRF-Chem model output shows that hydrocarbon emission ratios can be determined with good accuracy from concentrations at one location in the domain and by using calculated OH and ozone exposures to separate the effects of emissions, chemical removal, mixing, and transport. While the analysis as such was not done to evaluate how well the model describes the observations, it is clear that useful insights can be obtained from such detailed analysis of model output. For example, it was found that hydrocarbon and CO sources in the model are not as tightly coupled as in the atmosphere, which is not surprising since different emission inventories were used for hydrocarbons and CO. It is very encouraging that the OH exposure estimated from the measurements and model, and the relative importance of OH, NO_3, and ozone reactions are all in close agreement.

3.4. Comparison of Alkene Emissions With Other Studies

The emission ratios of alkenes versus CO, obtained in this work, are compared with the results from other studies in Figures 10 and S23. Included in these graphs are the following: (1) two studies that summarized extensive data sets of hydrocarbon measurements in urban air (Baker et al., 2008; Schneidemesser et al., 2010); (2) three studies that used hydrocarbon measurements in, respectively, the northeastern U.S., Beijing, and Paris to determine emission ratios versus CO after accounting for chemical removal (Borbon et al., 2013; Warneke et al., 2007; Yuan et al., 2012); (3) three tunnel studies that characterized hydrocarbon emissions from motor vehicles (Gentner et al., 2013; Kirchstetter, Singer, Harley, Kendall, & Hesson, 1999; Kirchstetter, Singer, Harley, Kendall, & Traverse, 1999; Lough et al., 2005); and (4) a dynamometer study that reported hydrocarbon emissions from motor vehicles (May et al., 2014). A second dynamometer study did not report CO emissions and was not included in Figure 10 (Schauer et al., 2002).

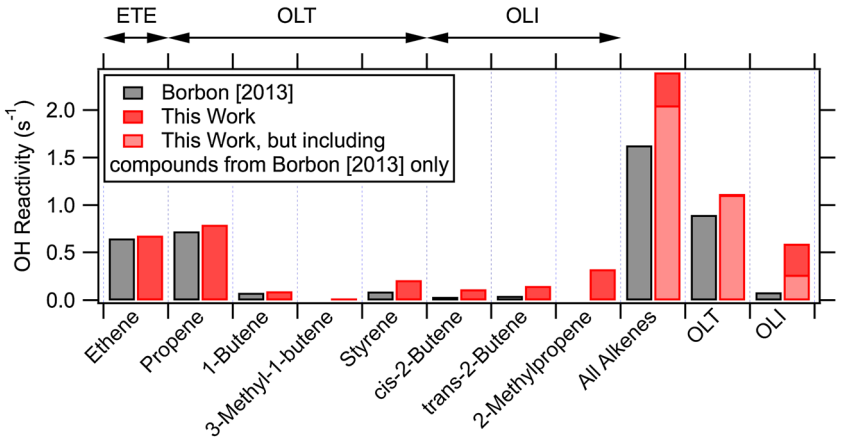

Figure 11. Comparison of alkene reactivity with OH using the previously reported emission ratios (Borbon et al., 2013) and the revised emission ratios reported in this work. OH reactivity is calculated using a daytime average CO mixing ratio of 300 ppbv. The present work both expanded on the number of reported alkenes, and revised the emission ratios of a few alkenes upward. The light red columns represent the combined OH reactivity of compounds that were included in the Borbon et al. (2013) study, but with revised emission ratios.

Alkene emission ratios versus CO vary significantly between the different studies (Figures 10a–10c). However, the same variability is observed for different alkenes. For example, Figure 10d shows a scatterplot of propene versus ethene emission ratios from the different studies and a high degree of correlation is found ($r^2 = 0.920$). A similar result is obtained for 1-butene, in which case the data point from the study in Beijing deviates significantly from the general trend (Figure S24). Therefore, the relative composition of alkene emissions appears to be much more similar between studies than the emission ratios versus CO, and alkene versus alkene ratios may be a better metric to compare in future work. Other studies have also reported regional differences in NMHC versus CO emission ratios, as well as long-term trends in these ratios (McDonald et al., 2013).

Emission ratios for all alkenes are compared with those from a detailed and recent dynamometer study at the California Air Resources Board Haagen-Smit and Heavy-Duty Engine Testing Laboratories (May et al., 2014). On average, the emission ratios reported here are 67% higher than those from the dynamometer study (Figure 10e), but the present results correlate closely with the dynamometer results. In other words, the composition of alkene emissions determined from the ambient data closely resembles that of motor vehicle emissions. The exceptions are isoprene and styrene. In the case of isoprene, it is likely that the discrepancy is caused by biogenic emissions, which overwhelm any anthropogenic sources during the day. The isoprene emission ratio was determined from nighttime data only when isoprene showed similar correlations with CO as other reactive alkenes (Figure 2c). Nevertheless, some of the isoprene that is emitted during the day can persist into the night (Brown et al., 2009). Other sources of styrene and isoprene include their use as precursors for industrial production of plastics and synthetic rubber. Isoprene is also one of the most common hydrocarbons in people's breath (King et al., 2010).

Alkene emissions from the dynamometer study by (May et al., 2014) were also compared with the results from three other tunnel studies (Gentner et al., 2013; Kirchstetter, Singer, Harley, Kendall, & Hesson, 1999; Kirchstetter, Singer, Harley, Kendall, & Traverse, 1999; Lough et al., 2005) and one other dynamometer study (Schauer et al., 2002). Results are presented in Figure S25. For the studies by Gentner et al. (2013), Kirchstetter, Singer, Harley, Kendall, and Hesson (1999), Kirchstetter, Singer, Harley, Kendall, and Traverse (1999), and Schauer et al. (2002), the composition of the alkene emissions show satisfactory agreement with May et al. (2014) with some notable exceptions. The exceptions are different for each comparison and do not seem to point at systematically under- or over-reported emissions in the May et al. (2014) study. In the study by Lough et al. (2005), the alkenes with lower emissions are systematically higher than the results from May et al. (2014) by as much as a factor of 100. The reasons for these discrepancies are unknown.

3.5. Implications for Ozone Formation

Alkenes provide a relatively large fraction of hydrocarbon reactivity in urban air and are among the most important precursors for ozone formation in urban air (Carter, 1994; Derwent et al., 1996). This work

added two alkenes to our previous analysis (2-methylpropene and 3-methyl-1-butene) (Borbon et al., 2013) and revised the emissions of some highly reactive alkenes upward (Figure 7b). Overall, this increased the OH reactivity of the emissions of reported alkenes by 47% (Figure 11; 26% if only compounds are considered that were included in both studies). For the terminal olefins (OLT), the OH reactivity increased by 25% (23% for compounds included in both studies). For the olefins with internal bonds (OLI), the OH reactivity increased by a factor of 7.0 (factor of 3.2 for compounds in both studies). These are significant increases that will affect modeled ozone production. Not all the alkenes that contribute significantly to OH reactivity were measured. Notably, 2-methyl-2-butene, 2-methyl-1-butene and trans-2-pentene are highly reactive with OH, and have significant emissions based on dynamometer studies (May et al., 2014), but were not measured in this study. These compounds are also highly reactive with ozone and NO_3. As a result, their ambient mixing ratios at night can be expected to be strongly reduced by chemical removal, and determining their emission ratios would be subject to the same issues as reported here for cis-2-butene and trans-2-butene.

The nighttime chemistry of anthropogenic alkenes is not expected to have a strong effect on the loss of NO_x at night. In most air masses, the loss of NO_3 to aerosol (via N_2O_5 uptake) and/or the reaction of NO_3 with biogenic VOCs are much larger sinks than the reaction with anthropogenic alkenes (Brown et al., 2009; Warneke et al., 2004). Nighttime reactions of alkenes with ozone and NO_3 lead to aldehyde formation at night. These processes will be studied in a later publication.

4. Conclusion

We reanalyzed a hydrocarbon data set obtained at a surface site in the Los Angeles basin during the 2010 CalNex study. While the removal of most alkanes, small alkenes, and aromatics was governed by OH chemistry, it is shown that nighttime removal of highly reactive alkenes by ozone and NO_3 was also significant. This nighttime removal complicates the determination of emission ratios versus CO from the measurements. Analogously to the determination of OH exposure from hydrocarbon ratios, we estimated the nighttime exposure to ozone and used this parameter to estimate emission ratios for highly reactive alkenes. The resulting emission ratios were up to a factor of 3 larger than previously reported values from the same data set. These findings suggest that other studies aimed at describing reactive alkene emissions must also account for nighttime removal by ozone and NO_3.

We evaluated our methods for data analysis by using model output for hydrocarbons and oxidants at the measurement location from the chemistry-transport model WRF-Chem. It was found that many of the features obtained from the measurements on hydrocarbon emissions and chemical removal were reproduced by the model. The emission ratios determined from the model output, using the same methods used to analyze the measurement data, agreed with the ratio between hydrocarbon and CO emissions in the domain centered on Pasadena in the model. Importantly, the agreement between emission ratios estimated from the model output and the actual emissions holds regardless of the hydrocarbon reactivity, showing that emissions and chemical removal can be separated using the methods used here. We compared the composition of alkene emissions with those from other ambient, tunnel, and dynamometer studies and found generally good agreement with a few notable exceptions. This demonstrates that motor vehicle emissions are the main sources of alkenes in the Los Angeles basin.

Acknowledgments
Data used in this study can be found at http://www.esrl.noaa.gov/csd/projects/calnex/. We gratefully acknowledge support from the California Institute of Technology and John Seinfeld for hosting the ground site during CalNex. Funding from the California Air Resources Board for the site infrastructure is greatly appreciated. Si-Wan Kim acknowledges support from the NASA ROSES ACMAP program (NNH14AX01I). The OH measurements were supported by grants from the National Science Foundation (AGS-0612738 and AGS-1104880). The NO_3 measurements were supported by a grant from the California Air Resources Board (ARB 08-318). One of us (J.d.G.) was associated with Aerodyne Research Inc. as a consultant during part of the preparation phase of the manuscript.

References

Ahmadov, R., McKeen, S., Trainer, M., Banta, R., Brewer, A., Brown, S., … Pétron, G. (2015). Understanding high wintertime ozone pollution events in an oil and natural gas-producing region of the western US. *Atmospheric Chemistry and Physics*, *15*, 411–429. https://doi.org/10.5194/acpd-14-20295-2014

Aschmann, S. M., & Atkinson, R. (2011). Effect of structure on the rate constants for reaction of NO3 radicals with a series of linear and branched C_5-C_7 1-alkenes at 296 ± 2 K. *The Journal of Physical Chemistry. A*, *115*(8), 1358–1363. https://doi.org/10.1021/jp111078u

Atkinson, R. (1986). Kinetics and mechanisms of the gas-phase reactions of the hydroxyl radical with organic compounds under atmospheric conditions. *Chemical Reviews*, *86*(1), 69–201. https://doi.org/10.1021/cr00071a004

Atkinson, R., & Arey, J. (2003). Atmospheric degradation of volatile organic compounds. *Chemical Reviews*, *103*, 4605–4638.

Baker, A. K., Beyersdorf, A. J., Doezema, L. A., Katzenstein, A., Meinardi, S., Simpson, I. J., … Rowland, F. S. (2008). Measurements of nonmethane hydrocarbons in 28 United States cities. *Atmospheric Environment*, *42*, 170–182.

Borbon, A., Fontaine, H., Veillerot, M., Locoge, N., Galloo, J. C., & Guillermo, R. (2001). An investigation into the traffic-related fraction of isoprene at an urban location. *Atmospheric Environment*, *35*, 3749–3760.

Borbon, A., Gilman, J. B., Kuster, W. C., Grand, N., Chevaillier, S., Colomb, A., … de Gouw, J. A. (2013). Emission ratios of anthropogenic volatile organic compounds in northern mid-latitude megacities: Observations versus emission inventories in Los Angeles and Paris. *Journal of Geophysical Research: Atmospheres*, *118*, 2041–2057. https://doi.org/10.1002/jgrd.50059

Brown, S. S., deGouw, J. A., Warneke, C., Ryerson, T. B., Dubé, W. P., Atlas, E., … Ravishankara, A. R. (2009). Nocturnal isoprene oxidation over the Northeast United States in summer and its impact on reactive nitrogen partitioning and secondary organic aerosol. *Atmospheric Chemistry and Physics*, *9*, 3027–3042.

Carter, W. P. L. (1994). Development of ozone reactivity scales for volatile organic compounds. *Journal of the Air & Waste Management Association*, *44*, 881–899.

Chan, A. W. H., Issacman, G., Wilson, K. R., Worton, D. R., Ruehl, C. R., Nah, T., … Goldstein, A. H. (2013). Detailed chemical characterization of unresolved complex mixtures (UCM) in atmospheric organics: Insights into emission sources, atmospheric processing and secondary organic aerosol formation. *Journal of Geophysical Research: Atmospheres*, *118*, 6783–6796. https://doi.org/10.1002/jgrd.50533

de Gouw, J. A., McKeen, S. A., Aikin, K. C., Brock, C. A., Brown, S. S., Gilman, J. B., … Wolfe, G. M. (2015). Airborne measurements of the atmospheric emissions from a fuel ethanol refinery. *Journal of Geophysical Research: Atmospheres*, *120*, 4385–4397. https://doi.org/10.1002/2015JD023138

de Gouw, J. A., Middlebrook, A. M., Warneke, C., Goldan, P. D., Kuster, W. C., Roberts, J. M., … Bates, T. S. (2005). Budget of organic carbon in a polluted atmosphere: Results from the New England Air Quality Study in 2002. *Journal of Geophysical Research*, *110*, D16305. https://doi.org/10.1029/2004JD005623

de Gouw, J. A., Te Lintel Hekkert, S., Mellqvist, J., Warneke, C., Atlas, E. L., Fehsenfeld, F. C., … Zhu, X. (2009). Airborne measurements of ethene from industrial sources using laser photo-acoustic spectroscopy. *Environmental Science & Technology*, *43*, 2437–2442.

Derwent, R. G., Jenkin, M. E., & Saunders, S. M. (1996). Photochemical ozone creation potentials for a large number of reactive hydrocarbons under European conditions. *Atmospheric Environment*, *30*, 181–199.

Emmons, L. K., Walters, S., Hess, P. G., Lamarque, J.-F., Pfister, G. G., Fillmore, D., … Kloster, S. (2010). Description and evaluation of the Model for Ozone and Related chemical Tracers, version 4 (MOZART-4). *Geoscientific Model Development*, *3*, 43–67.

Ensberg, J. J., Hayes, P. L., Jimenez, J. L., Gilman, J. B., Kuster, W. C., de Gouw, J. A., … Seinfeld, J. H. (2014). Emission factor ratios, SOA mass yields, and the impact of vehicular emissions on SOA formation. *Atmospheric Chemistry and Physics*, *14*, 2383–2397.

Gentner, D. R., Worton, D. R., Isaacman, G., Davis, L. C., Dallmann, T. R., Wood, E. C., … Harley, R. A. (2013). Chemical composition of gas-phase organic carbon emissions from motor vehicles and implications for ozone production. *Environmental Science & Technology*, *47*, 11,837–11,848.

Gerbig, C., Smitgen, S., Kley, D., Volz-Thomas, A., Dewey, H., & Haaks, D. (1999). An improved fast response vacuum UV resonance fluorescence CO instrument. *Journal of Geophysical Research*, *104*, 1699–1704.

Gilman, J. B., Burkhart, J. F., Lerner, B. M., Williams, E. J., Kuster, W. C., Goldan, P. D., … de Gouw, J. A. (2010). Ozone variability and halogen oxidation within the Arctic and sub-Arctic springtime boundary layer. *Atmospheric Chemistry and Physics*, *10*, 10,223–10,236.

Grell, G. A., Peckham, S. E., Schmitz, R., McKeen, S. A., Frost, G., Skamarock, W. C., & Eder, B. (2005). Fully coupled "online" chemistry within the WRF model. *Atmospheric Environment*, *39*, 6957–6975. https://doi.org/10.1016/j.atmosenv.2005.04.027

Griffin, R., Chen, J., Carmody, K., Vutukuru, S., & Dabdub, D. (2007). Contribution of gas phase oxidation of volatile organic compounds to atmospheric carbon monoxide levels in two areas of the United States. *Journal of Geophysical Research*, *112*, D10S17. https://doi.org/10.1029/2006JD007602

Griffith, S. M., Hansen, R. F., Dusanter, S., Michoud, V., Gilman, J. B., Kuster, W. C., … Stevens, P. S. (2016). Measurements of hydroxyl and hydroperoxy radicals during CalNex-LA: Model comparisons and radical budgets. *Journal of Geophysical Research: Atmospheres*, *121*, 4211–4232. https://doi.org/10.1002/2015JD024358

Hayes, P. L., Ortega, A. M., Cubison, M. J., Froyd, K. D., Zhao, Y., Cliff, S. S., … Jimenez, J. L. (2013). Aerosol composition and sources in Pasadena, California during the 2010 CalNex campaign. *Journal of Geophysical Research: Atmospheres*, *118*, 9233–9257. https://doi.org/10.1002/jgrd.50530

Karl, T., Apel, E. C., Hodzic, A., Riemer, D. D., Blake, D. R., & Wiedinmyer, C. (2009). Emissions of volatile organic compounds inferred from airborne flux measurements over a megacity. *Atmospheric Chemistry and Physics*, *9*, 271–285.

Kim, S.-W., Heckel, A., Frost, G. J., Richter, A., Gleason, J., Burrows, J. P., … Trainer, M. (2009). NO2 columns in the western United States observed from space and simulated by a regional chemistry model and their implications for NO_x emissions. *Journal of Geophysical Research*, *114*, D11301. https://doi.org/10.1029/2008JD011343

Kim, S.-W., McDonald, B. C., Baidar, S., Brown, S. S., Dube, B., Ferrance, R. A., … Young, C. J. (2016). Modeling the weekly cycle of NO*x* and CO emissions and their impacts on O_3 in the Los Angeles-South Coast Air Basin during the CalNex 2010 field campaign. *Journal of Geophysical Research: Atmospheres*, *121*, 1340–1360. https://doi.org/10.1002/2015JD024292

King, J., Koc, H., Unterkofler, K., Mochalski, P., Kupferthaler, A., Teschl, G., … Amann, A. (2010). Physiological modeling of isoprene dynamics in exhaled breath. *Journal of Theoretical Biology*, *267*, 626–637.

Kirchstetter, T. W., Singer, B. C., Harley, R. A., Kendall, G. R., & Hesson, J. M. (1999). Impact of California reformulated gasoline on motor vehicle emissions. 2. Volatile organic compound speciation and reactivity. *Environmental Science & Technology*, *33*, 329–336.

Kirchstetter, T. W., Singer, B. C., Harley, R. A., Kendall, G. R., & Traverse, M. (1999). Impact of California reformulated gasoline on motor vehicle emissions. 1. Mass emission rates. *Environmental Science & Technology*, *33*, 318–328. https://doi.org/10.1021/es9803714

Lerner, B. M., Gilman, J. B., Aikin, K. C., Atlas, E. L., Goldan, P. D., Graus, M., … de Gouw, J. A. (2017). An improved, automated whole-air sampler and gas chromatography mass spectrometry analysis system for volatile organic compounds in the atmosphere. *Atmospheric Measurement Techniques*, *10*, 291–313.

Lough, G. C., Schauer, J. J., Lonneman, W. A., & Allen, M. K. (2005). Summer and winter nonmethane hydrocarbon emissions from on-road motor vehicles in the midwestern United States. *Journal of the Air & Waste Management Association (1995)*, *55*, 629–646.

May, A. A., Nguyen, N. T., Presto, A. A., Gordon, T. D., Lipsky, E. M., Karve, M., … Robinson, A. L. (2014). Gas- and particle-phase primary emissions from in-use, on-road gasoline and diesel vehicles. *Atmospheric Environment*, *88*, 247–260.

McDonald, B. C., Dallmann, T. R., Martin, E. W., & Harley, R. A. (2012). Long-term trends in nitrogen oxide emissions from motor vehicles at national, state, and air basin scales. *Journal of Geophysical Research*, *117*, D00V18, https://doi.org/10.1029/2012JD018304

McDonald, B. C., Gentner, D. R., Goldstein, A. H., & Harley, R. A. (2013). Long-term trends in motor vehicle emissions in U.S. urban areas. *Environmental Science & Technology*, *47*, 10,022–10,031.

McDonald, B. C., McBride, Z. C., Martin, E. W., & Harley, R. A. (2014). High-resolution mapping of motor vehicle carbon dioxide emissions. *Journal of Geophysical Research: Atmospheres*, *119*, 5283–5298. https://doi.org/10.1002/2013JD021219

Miller, S. M., Matross, D. M., Andrews, A. E., Millet, D. B., Longo, M., Gottlieb, E. W., … Wofsy, S. C. (2008). Sources of carbon monoxide and formaldehyde in North America determined from high-resolution atmospheric data. *Atmospheric Chemistry and Physics*, *8*, 7673–7696.

Odum, J. R., Jungkamp, T. P. W., Griffin, R., Flagan, R. C., & Seinfeld, J. H. (1997). The atmospheric aerosol-forming potential of whole gasoline vapor. *Science*, *276*, 96–99.

Parrish, D. D., Ryerson, T. B., Mellqvist, J., Johansson, J., Fried, A., Richter, D., … Herndon, S. C. (2012). Primary and secondary sources of formaldehyde in urban atmospheres: Houston Texas region. *Atmospheric Chemistry and Physics*, *12*, 3273–3288.

Peischl, J., Ryerson, T. B., Brioude, J., Aikin, K. C., Andrews, A. E., Atlas, E., … Parrish, D. D. (2013). Quantifying sources of methane and light alkanes in the Los Angeles Basin, California. *Journal of Geophysical Research: Atmospheres*, *118*, 4974–4990. https://doi.org/10.1002/jgrd.50413

Petron, G., Forst, G., Miller, B. R., Hirsch, A. I., Montzka, S. A., Karion, A., … Tans, P. (2012). Hydrocarbon emissions characterization in the Colorado Front Range: A pilot study. *Journal of Geophysical Research*, *117*, D04304. https://doi.org/10.1029/2011JD016360

Pollack, I. B., Ryerson, T. B., Trainer, M., Parish, D. D., Andrews, A. E., Atlas, E. L., … Xiang, B. (2012). Airborne and ground-based observations of a weekend effect in ozone, precursors, and oxidation products in the California South Coast Air Basin. *Journal of Geophysical Research*, *117*, D00V05. https://doi.org/10.1029/2011JD016772

Riedel, T. P., Bertram, T. H., Crisp, T. A., Williams, E. J., Lerner, B. M., Vlasenko, A., … Thornton, J. A. (2012). Nitryl chloride and molecular chlorine in the coastal marine boundary layer. *Environmental Science & Technology*, *46*, 10,463–10,470.

Ryerson, T. B., Trainer, M., Angevine, W. M., Brock, C. A., Dissly, R. W., Fehsenfeld, F. C., … Senff, C. J. (2003). Effect of petrochemical industrial emissions of reactive alkenes and NO_x on tropospheric ozone formation in Houston, Texas. *Journal of Geophysical Research*, *108*, 4249. https://doi.org/10.1029/2002JD003070

Schauer, J. J., Kleeman, M. J., Cass, G. R., & Simoneit, B. R. T. (2002). Measurement of emissions from air pollution sources. 5. C_1-C_{32} organic compounds from gasoline-powered motor vehicles. *Environmental Science & Technology*, *36*, 1169–1180.

Schneidemesser, E. V., Monks, P. S., & Plass-Duelmer, C. (2010). Global comparison of VOC and CO observations in urban areas. *Atmospheric Environment*, *44*, 5053–5064.

Scott, K. I., & Benjamin, M. T. (2003). Development of a biogenic volatile organic compounds emission inventory for the SCOS97-NARSTO domain. *Atmospheric Environment*, *37*, 39–49. https://doi.org/10.1016/S1352-2310(03)00381-9

Sprengnether, M. M., Demerjian, K. L., Dransfield, T. J., Clarke, J. S., Anderson, J. G., & Donahue, N. M. (2009). Rate constants of nine C_6-C_9 alkanes with OH from 230 to 379 K: Chemical tracers for [OH]. *The Journal of Physical Chemistry. A*, *113*(17), 5030–5038. https://doi.org/10.1021/jp810412m

Stockwell, W. R., Kirchner, F., & Kuhn, M. (1997). A new mechanism for regional atmospheric chemistry modeling. *Journal of Geophysical Research*, *102*, 25,847–25,879.

Tsai, C., Wong, C., Hurlock, S., Pikelnaya, O., Mielke, L. H., Osthoff, H. D., … Stutz, J. (2014). Nocturnal loss of NO_x during the 2010 CalNex-LA study in the Los Angeles Basin. *Journal of Geophysical Research: Atmospheres*, *119*, 13,004–13,025. https://doi.org/10.1002/2014JD022171

Warneke, C., de Gouw, J. A., Goldan, P. D., Kuster, W. C., Williams, E. J., Lerner, B. M., … Fensenfeld, F. C. (2004). Comparison of daytime and nighttime oxidation of biogenic and anthropogenic VOCs along the New England coast in summer during New England Air Quality Study 2002. *Journal of Geophysical Research*, *109*, D10309. https://doi.org/10.1029/2003JD004424

Warneke, C., de Gouw, J. A., Edwards, P. M., Holloway, J. S., Gilman, J. B., Kuster, W. C., … Parrish, D. D. (2013). Photochemical aging of volatile organic compounds in the Los Angeles basin: Weekday-weekend effect. *Journal of Geophysical Research: Atmospheres*, *118*, 5018–5028. https://doi.org/10.1002/jgrd.50423

Warneke, C., McKeen, S. A., de Gouw, J. A., Goldan, P. D., Kuster, W. C., Holloway, J. S., … Blake, D. R. (2007). Determination of urban volatile organic compound emission ratios and comparison with an emissions database. *Journal of Geophysical Research*, *112*, D10S47. https://doi.org/10.1029/2006JD007930

Young, C. J., Washenfelder, R. A., Roberts, J. M., Mielke, L. H., Osthoff, H. D., Tsai, C., … Brown, S. S. (2012). Vertically resolved measurements of nighttime radical reservoirs in Los Angeles and their contribution to the urban radical budget. *Environmental Science & Technology*, *46*, 10,965–10,973.

Yuan, B., Shao, M., de Gouw, J., Parrish, D. D., Lu, S., Wang, M., … Hu, M. (2012). Volatile organic compounds (VOCs) in urban air: How chemistry affects the interpretation of positive matrix factorization (PMF) analysis. *Journal of Geophysical Research*, *117*, D24302. https://doi.org/10.1029/2012JD018236

Zhao, Y., Hennigan, C. J., May, A. A., Tkacik, D. S., de Gouw, J. A., Gilman, J. B., … Robinson, A. L. (2014). Intermediate-volatility organic compounds: A large source of secondary organic aerosol. *Environmental Science & Technology*, *48*, 13,743–13,750.